6-15-2007

Information Surfing for Model-driven Radiation Mapping

Andres Cortez

Herbert G. Tanner

DEPARTMENT OF MECHANICAL ENGINEERING

THE UNIVERSITY of NEW MEXICO

Information Surfing for Model-driven Radiation Mapping

Andres R. Cortez and Herbert G. Tanner [1]
Department of Mechanical Engineering
The University of New Mexico
Albuquerque, NM 87131

UNM Technical Report: ME-TR-07-001

Report Date: June 13, 2007

[1] Supported by DoE URPR grant DE-FG52-04NA25590

Abstract

In this report we develop a control scheme to coordinate a group of mobile sensors for radiation mapping of a given planar polygon region. The control algorithm is based on the concept of *information surfing*, where navigation is done by means of following information gradients, taking into account sensing performance as well as inter-robot communication range limitations. The control scheme provably steers mobile sensors to locations at which they maximize the information content of their measurement data, and the asymptotic properties of our information metric with respect to time ensures that no local information metric extremum traps the sensors indefinitely. In addition, the inherent synergy of the mobile sensor group facilitates the temporal "erosion" of such extremum configurations. Information surfing allows for reactive mobile sensor network behavior and adaptation to environmental changes, as well as human retasking.

Keywords

Information surfing, mobile sensor networks, radiation mapping

1 Introduction

Imagine there is a nuclear contamination of a large metropolitan area. How big is the contaminated area? How dangerous is the radiation being emitted from this contamination? The sooner these questions can be answered, the faster the situation can be assessed. The ability to address these issues could save lives, facilitate decontamination efforts, and yield economic savings. Current technology in radiation detection is not well suited for this type of scenario. A group of robots can provide situational awareness by cooperating with each other to map the contaminated area. With a radiation map of the area, decision makers are able to better assess the extent of the problem and handle the situation more efficiently. To be successful in this mission, robots need a method of coordinating their actions in a way that allows for rapid mapping of the contaminated area at a progressively higher level of accuracy. Using large teams of robots, we avoid placing humans in harm's way and we quickly map big areas.

The goal of our work is to design a control algorithm for a group of cooperating robots to map the radiation levels over an area of interest. The control scheme should be decentralized, in order to be implementable with an effort that scales with the size of the group. It should take into account the performance of the sensors and inter-robot communication limitations.

We approach this problem by breaking up the area to be mapped among the team members. This partitioning of the area is dynamic, because it depends on the locations of the robots. The partitioning of the region is updated after a robot reaches a new position. The robots follow information gradients and with new data collected they continuously update their map. After obtaining a map of the area at a desired level of accuracy, the mission is completed. Because this map is continuously updated, a real-time snapshot can be generated at any time and thus situational awareness is provided at different confidence levels, even from the first minute.

With relatively inexpensive and capable hardware in communication, computing, and sensing, as well as the many practical applications, research in cooperative control of mobile robots has become a big area in controls research. Applications can be found in coordination of robots for topological mapping (Burgard et al., 2000; Thrun, 2001; Grabowski et al., 2000). Burgard et al. (2000) use target points to coordinate the team of robots. A target point is chosen by weighing the cost and utility of each target point. Thrun (2001) extends region *frontiers*, defined based on information-theoretic considerations, to achieve the underlying coordination of the group. Frontiers are regions that are on the boundaries of the area which has been explored and the region which is unexplored. Grabowski et al. (2000) use occupancy grids with a Bayesian update rule to coordinate the group for topological mapping. In an occupancy grid, the environment is divided into homogeneous cells that contain a probability of being occupied by an obstacle. Another application in cooperative control is found in robotic deployment of sensor networks (Popa et al., 2004; Martinez et al., 2007; Cortes et al., 2005; Hussein and Stipanovic, 2006). Popa et al. (2004) take advantage of potential fields to achieve the desired motion of the group. Potential fields place artificial forces on the agents, and through these forces the desired trajectories are obtained. Martinez et al. (2007) and Cortes et al. (2005) use gradient climbing algorithms to distribute agents in an optimal fashion over the area in question. Agents follow gradients that maximize a static density function that is weighted by a sensor performance function. Hussein and Stipanovic (2006) use a gradient climbing method for control of the group as well, but does so without having to partition the area among the team members, which reduces computational overhead.

Coordination algorithms for robots deployed for topological mapping, typically assume ideal sensors. However, it is unlikely that approaches assuming ideal sensors can be implemented in the field without significant concessions in terms of performance of the sensors. Most of the work in sensor network deployment, usually relies on prior information to coordinate the sensors. This information is static, therefore if the environment changes these approaches are unable to adapt easily to reconfigure in an optimized fashion.

Most approaches to navigation for groups of robots fall under the category of gradient following (Orgen et al., 2004; Lindhe et al., 2005; Cortes and Bullo, 2005), "frontier-based" approach (Moorehead, 2001; Yamauchi, 1998), or occupancy grids Elfes (1989); Moravec (1988); Lilienthal and Duckett (2004). The gradient following approach, mostly concentrates on sensor coverage, where the group is initially in a random configuration and the

control algorithm coordinates the group to an optimal configuration in the sense of sensor coverage. This method is suited to surveillance applications. In the frontier-based approach, the agents move to the boundary of the area which has been explored and the region which is unexplored. Successively doing this allows for the whole area to be explored. This type of approach assume that the explored area is completely known after the area is explored. This approach is not reactive to changes in the environment, because once a region is scanned it is assumed to be completely known. It does not allows for addressing the question of whether an area should be scanned again. With the occupancy grid approach, the area to be investigated is partitioned into cells that contain the probabilities of the cell being occupied by an obstacle. Path planning can then be made based on cost metrics of paths through these cells. Much like the frontier-based approach, navigation of the agents is done in a way to quickly visit all cells within the area, rather than investigate the most "interesting" regions.

Most of the research in navigation for groups of robots assumes a static, time-invariant environment. Because of this, a good model of the environment is required. In application like the one considered in this paper, this assumption is not realistic. Furthermore, most approaches to group navigation are not reactive with respect to the sensed environment, and therefore unable to cope with a dynamic environment. One exception is the work of Grocholsky et al. (2006), where the control of the group is done in a way to reduce state estimate uncertainty. This type of navigation is named *information surfing*, because agents are driven to maximize their information gain. Our approach is similar in spirit, but whereas Grocholsky et al. (2006) perform *information surfing* for topological mapping and surveillance, in this report it is applied to radiation map building. The main differences are the underlying measurement statistics and the time-varying nature of the optimization objective considered here. In addition, we provide a mathematical proof of convergence to "interesting configurations" and we indicate how our closed loop system is capable of avoiding getting stuck at singular configurations.

The latter theoretical result needs to be emphasized, because most of the work in this area lacks completeness in the sense of stability of the control algorithm and the asymptomatic behavior of the group. In this report we focus on establishing the stability of the coordination algorithm when a time varying information gradient is used. The outcome is a cooperative motion and measurement strategy that provides real time situational awareness which is a key tool in helping assess and react to the problem at hand.

2 Problem Statement

For this scenario we assume n holonomic robots, equipped with radiation sensors and capable of omnidirectional motion. Each robotic agent in the group is assumed to be described kinematically as a single integrator. Therefore, if p_i indicates the planar coordinates of the ith robot, then $\dot{p}_i = u_i$, where u_i is its control input. Stacking all robot coordinates and inputs to two corresponding vectors $\mathbf{p}$ and $\mathbf{u}$, we obtain

$$\dot{\mathbf{p}} = \mathbf{u}. \tag{1}$$

Each robot is assumed to be able to communicate with its neighboring robots. Its radiation sensor is capable of measuring radiation counts from source activities α, in the range $\alpha_1 \leq \alpha \leq \alpha_2$.

The area to be mapped for radiation is a a simple convex polygon, $Q \in \mathbb{R}^2$. Each robot has prior knowledge of the boundaries of Q. A layout of the configuration for the proposed investigation is shown in Figure 1.

The problem that we address can be expressed as follows:

Problem 2.1. *Develop a decentralized control strategy for the deployment and coordination of a mobile robot team, to create a radiation map of a convex polygon. The coordination algorithm should account for sensor performance limitations as well as communication restrictions within the group.*

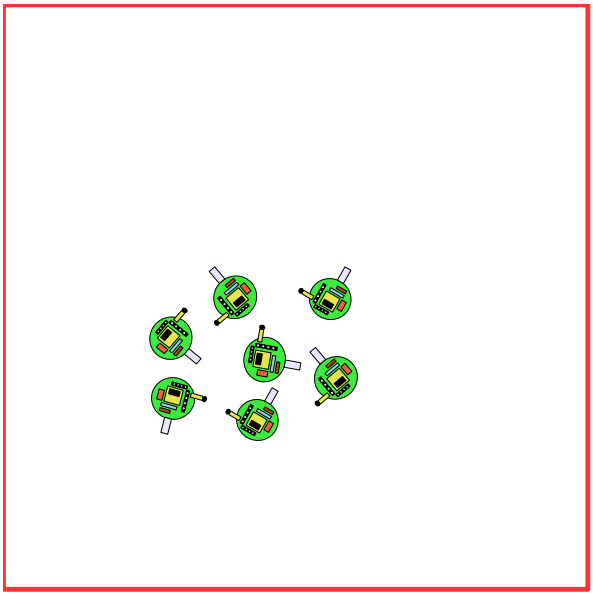

Figure 1: The layout of the proposed area to be searched with a team of robots in a random configuration. Each robot is equipped with radiation sensors as well as radio communication. These robots are actually non holonomic, and holonomic motion can be approximated in two steps: rotation in place, then straight line motion.

3 The Probabilistic Dynamics of Radiation Measurements

Low-rate counting of radiation from nuclear decay is described by the Poisson statistics, where the probability to register n counts in t seconds, from a source assumed to emit an average of μ counts per second (cts/s) is

$$P(n,t) = \frac{(\mu \cdot t)^n}{n!} e^{-(\mu \cdot t)}. \tag{2}$$

In Nemzek et al. (2004), the authors describe how to model radiation measurements from a moving source with a stationary sensor. In our approach we take that same idea but turn it around and look at a stationary source with a moving sensor. We can describe the expected number of source counts, μ, to be registered by a moving sensor as

$$\mu = \chi \cdot \alpha \int_0^t \frac{1}{r^2(t)} \, \mathrm{d}t \,, \tag{3}$$

where χ is the cross sectional area of the sensor, α is the activity of the source, and $r(t)$ is the instantaneous distance of the source to the sensor.

We can now describe the probability density function (PDF) associated with the random variable c, which is the total number of counts recorded, for a moving sensor as

$$f(c) = \frac{(\mu)^c}{c!} \cdot e^{-(\mu)}, \tag{4}$$

where μ is expressed in (3).

The expected number of counts μ is conditioned on the source having activity α, the cross sectional area of the sensor being χ, and the distance between the source and sensor being $r(t)$. Therefore the PDF associated with the random variable c is formally

$$f(c) = f(c|\alpha, \chi, r(t)). \tag{5}$$

In Cortez et al. (2007) it is seen that Bayes rule allows us to calculate $f(\alpha|c,\chi,r(t))$ using $f(c|\alpha,\chi,r(t))$. As new measurements are taken by the sensor, we update the distribution using the equation

$$f(\alpha|c,\chi,r(t)) = \frac{f(\alpha)\cdot f(c|\alpha,\chi,r(t))}{f_c(c)}. \tag{6}$$

Function $f(\alpha)$ is the PDF associated with having a source with activity α at a distance $r(t)$. In our formulation we take this to be the uniform distribution, from source activity α_1 to a source activity α_2. This allows us to search and map radiation levels from an arbitrary source with activity α, such that $\alpha_1 < \alpha < \alpha_2$. In fact, $f(\alpha)$ is a function of position too, but when assuming a uniform distribution, the position of the sensor does not matter. From this point, the PDF expressing our initial guess about the source activity will be expressed as

$$f(\alpha) = \begin{cases} \frac{1}{\alpha_2-\alpha_1}, & \text{if } \alpha_1 < \alpha < \alpha_2 \\ 0, & \text{otherwise.} \end{cases}. \tag{7}$$

Function $f_c(c)$ is the marginal density function of $f(c)$

$$f_c(c) = \int_{\alpha_1}^{\alpha_2} \left[\frac{(\chi\cdot\alpha\int_0^t \frac{1}{r^2(t)}\,\mathrm{d}t)^c}{c!} \cdot e^{-(\chi\cdot\alpha\int_0^t \frac{1}{r^2(t)}\,\mathrm{d}t)} \right] \mathrm{d}\alpha. \tag{8}$$

4 Differential Entropy and Mutual Information

Viewing our radiation sensor as a communication channel between the robot (receiver) and its environment (sender), we can introduce metrics to describe the transmission of information. An entropy-based metric provides an intuitive way of measuring how much information we gain by a given measurement. The entropy is also known as self information, and is related to uncertainty because as the latter decreases the information gain increases. By using such a measure we can formalize the objective of our control law as reducing the uncertainty of our belief regarding the radiation levels over the area of interest.

Information theory defines the conditional differential entropy of a continuous random variables A associated with the transmitted signal, (in our case the radiation source activity), and C associated with the received signal, (in our case the number of counts registered by our sensors) as follows,

$$h(A|C) = -\int_{\alpha_1}^{\alpha_2} f(\alpha|c)\cdot log_2 \cdot f(\alpha|c)\,\mathrm{d}\alpha. \tag{9}$$

Note that we are using the definition of the differential entropy for continuous distributions even though the Poisson distribution is discrete. This because our ultimate objective is to derive a continuous time/space control laws based on information gradients. Our workspace is continuous even if our measurement events are discrete.

Using (6), denoting the generalized hypergeometric function $\Omega(\cdot)$ and defining

$$d \triangleq \int_0^t \frac{1}{r^2(t)}\,\mathrm{d}t,$$

we get a closed form solution for the differential entropy in (9) as follows

$$h(A|C) = \frac{-d\cdot\chi}{[\Gamma(c+1,\alpha_1\cdot d\cdot\chi)-\Gamma(c+1,\alpha_2\cdot d\cdot\chi)]\log 2} \cdot\Bigg[\frac{c\cdot\Omega(c+1,c+1;c+2,c+2;-\alpha_1\cdot d\cdot\chi)(\alpha_1\cdot d\cdot\chi)^{c+1}-(c+1)^2\Gamma(c+2,\alpha_1\cdot d\cdot\chi)}{(c+1)^2 d\cdot\chi} \cdot\frac{c\cdot\Omega(c+1,c+1;c+2,c+2;-\alpha_2\cdot d\cdot\chi)(\alpha_2\cdot d\cdot\chi)^{c+1}-(c+1)^2\Gamma(c+2,\alpha_2\cdot d\cdot\chi)}{(c+1)^2 d\cdot\chi} \cdot\frac{(c+1)\Gamma(c+1,\alpha_1\cdot d\cdot\chi)(\alpha_1\cdot d\cdot\chi+\log(e^{-\alpha_1\cdot d\cdot\chi})(\alpha_1\cdot d\cdot\chi)^c)-c\cdot\Gamma(c+2)\log(\alpha_1)}{(c+1)^2 d\cdot\chi} \cdot\frac{-c\cdot\Gamma(c+2)\log(\alpha_2)+(c+1)\Gamma(c+1,\alpha_2\cdot d\cdot\chi)(\alpha_2\cdot d\cdot\chi+\log(e^{-\alpha_2\cdot d\cdot\chi})(\alpha_2\cdot d\cdot\chi)^c)}{(c+1)^2 d\cdot\chi}\Bigg] - \frac{\log\left(\frac{d\cdot\chi}{\Gamma(c+1,\alpha_1\cdot d\cdot\chi)-\Gamma(c+1,\alpha_2 d\cdot\chi)}\right)}{c!\log 2}, \quad (10)$$

Note that (10) is a time and position dependent quantity.

It is known that continuous differential entropy can not be directly associated with self-information – contrary to the discrete scheme (Reza, 1994). One concept that *does* carry over from the discrete setting is the *mutual information*

$$I(X;Y) \triangleq h(X) - h(X|Y).$$

Mutual information quantifies the mutual dependence of the two random variables, X and Y. It tells us how knowing one variable, Y, reduces our uncertainty about the other variable, X. We exploit the property of mutual information expressed in the following Lemma.

Lemma 4.1. *(Cover and Thomas (1991)) $I(X;Y) \geq 0$ with equality iff X and Y are independent.*

For our problem, the mutual information is defined as

$$I(A;C) = h(A) - h(A|C).$$

Where

$$h(A) = -\int_{\alpha_1}^{\alpha_2} f(\alpha)\,d\alpha = -\int_{\alpha_1}^{\alpha_2} \frac{1}{\alpha_2-\alpha_1}\cdot\log\left(\frac{1}{\alpha_2-\alpha_1}\right)d\alpha = (\alpha_2-\alpha_1)\left[\frac{1}{\alpha_2-\alpha_1}\cdot\log\left(\frac{1}{\alpha_2-\alpha_1}\right)\right] \triangleq K,$$

which is a constant. With $h(A|C)$ as in (10), mutual information is described as

$$I(A;C) = K - h(A|C). \quad (11)$$

Equation (11) expresses how knowing the number of radiation counts, reduces our uncertainty regarding the presence of the source A.

5 Planning Motion to Gather Information

In this section we describe how to dynamically partition the area based on each robots location and also define a function to gauge sensor performance. Combining sensor performance and mutual information over the partitioned area, we are able to describe our objective function. This objective function measures the mutual information weighted by the sensors performance.

Let Q be a simple convex polygon in $\mathbb{R}^2$ including its interior. Let P be a set of n distinct points $\{p_1, \ldots, p_n\}$. Define the *Voronoi Partition* generated by P to the convex polygon Q to be

$$V_i(P) = \{q \in Q \,|, \|q - p_i\| \leq \|q - p_j\| \, \forall p_j \in P\}.$$

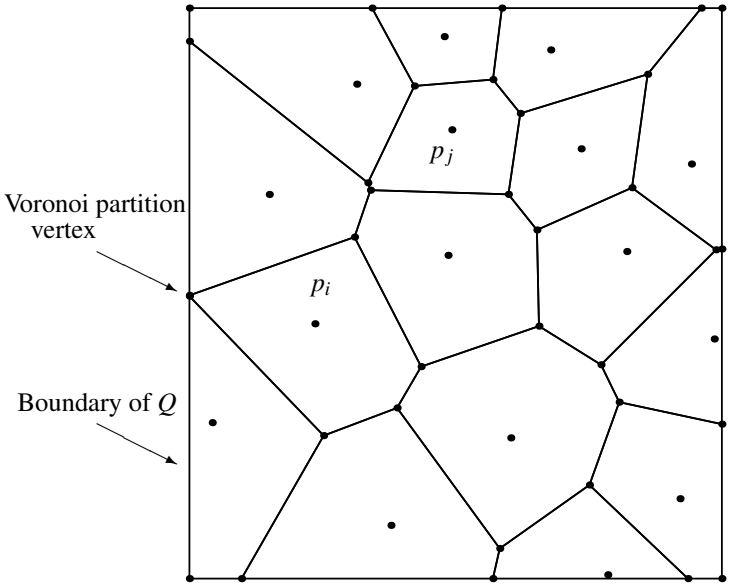

Figure 2: Example plot of Bounded Voronoi Partition. Our convex polygon is the rectangular boundary, and each dot which is not on the Voronoi partition (one of its vertices) represents a robot in its respective Voronoi cell.

Figure 2 shows how the convex polygon Q is partitioned by the Voronoi cells created by $V_i(P)$. To define the boundaries of its cell, robot i at position p_i only needs to know the boundary of Q and the positions of its nearest *neighbors*. A *neighbor* to robot i (in the sequel identified with its position p_i) is any other point p_j, such that the Voronoi cells of p_i and p_j share a common edge.

A *performance function* $f : \mathbb{R}_+ \to \mathbb{R}$ is a non-increasing and piecewise differentiable map with finite jump discontinuities, (Cortes et al., 2005). The performance function is a quantitative model of the signal-to-noise ratio (SNR) of our radiation sensor as a function of the distance of the sensor from the source. In nuclear search, the SNR falls as the distance R to the source increases proportionally to R^2 (Klimenko et al., 2006). Let us define the performance function as

$$f(\|q - p_i\|) = \begin{cases} \dfrac{\exp\left(\frac{-1}{(R^2 - \|q-p_i\|)}\right)}{\exp\left(\frac{-1}{(R^2 - \|q-p_i\|)}\right) + \exp\left(\frac{-1}{(\|q-p_i\| - R^2)}\right)} & \text{if } \frac{1}{2}R < \|q - p_i\| < R, \\ 1 & \text{if } 0 \leq \|q - p_i\| \leq \frac{1}{2}R, \\ 0 & \text{if } R \leq \|q - p_i\|. \end{cases} \tag{12}$$

Distance R is the sensor detection range which is considered to be a constant, and $\|q - p_i\|$ is the Euclidean distance from the sensor to the source. Constructing f in this manner ensures that $f(\|q - p_i\|)$ is continuously differentiable (Boothby, 1986). From Figure 3, it is seen that the performance function is identically equal to one for part of the sensing range. This limit is defined to be approximately 0.5. This is due to the geometry of the

sensor, where normally a perfect reading can be obtained along the whole length of the sensor, and not just at a particular point. By construction, $f(\|q-p_i\|) \geq 0 \,\forall\, p_i, q, \quad$ for $i = 1, \ldots, n$.

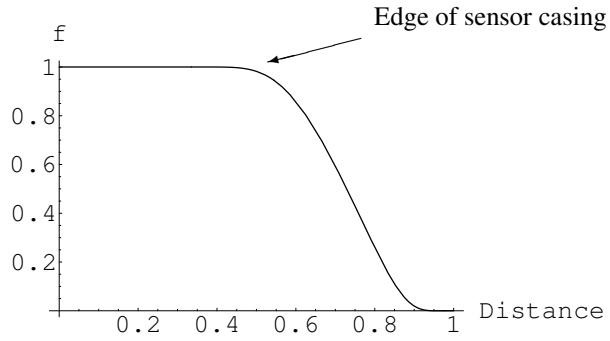

Figure 3: An example of the type of performance function considered for the radiation sensor used, assuming the length of the sensor protective casing to be 0.05 m.

The radiation mapping problem considered here falls in the category of multiple sensor coverage control because we are trying to place the robots in a configuration that is optimal with respect to information gained from sensors. This is very similar to the area covering problems in robot surveillance, where they are placed in a configuration to optimize there sensor coverage over the area. Most of the work in coverage control addresses the case where the environment to be covered is time invariant (static), as in (Cortes et al., 2005) where the goal is to maximize the following function

$$\mathcal{H}(P) = \int_{V_i(P)} f(\|q-p_i\|)\phi(q)\,\mathrm{d}q.$$

We focus our attention on a dynamic version of this problem, where the underlying density function ϕ is time dependent. The mutual information, $I(q,p_i,t)$ will play the role of density function for this problem. Let us define the objective function for the problem considered here as

$$\mathcal{W}(P) = \int_{V_i(P)} f(\|q-p_i\|)I(q,p_i,t)\,\mathrm{d}q. \tag{13}$$

6 Control Design and Stability Analysis

Assume that the kinematics of each robot i are simply described as

$$\dot{p}_i = u_i, \tag{14}$$

where u_i is the control input, designed to make the robot follow the gradient of mutual information in the following way

$$u_i = -\Big[\int_{V_i(P)} \frac{\partial f(\|q-p_i\|)}{\partial p_i} I(q,p_i,t)\mathrm{d}q + \int_{V_i(P)} f(\|q-p_i\|)\frac{\partial I(q,p_i,t)}{\partial p_i}\mathrm{d}q\Big]. \tag{15}$$

The following Lemma is used in the proof of our main result. The proof of this Lemma is given in Appendix A.

Lemma 6.1. *Let $I(q,p_i,t)$ be the mutual information of the radiation sensor information channel. Then,*

$$\lim_{t\to\infty} \frac{\partial I(q,p_i,t)}{\partial t} = 0.$$

Proposition 6.2. *Consider the gradient field defined by (14) –(15). Then the system stabilizes at configurations that (locally) minimize the information flow from each robot as expressed by the product $I(q,p_i,t)f(\|q-p_i\|)$, for $i=1,\ldots,n$.*

Proof. Notice that

$$\frac{\partial(I(q,p_i,t)\,f(\|q-p_i\|)}{\partial p_i} = \frac{\partial f(\|q-p_i\|)}{\partial p_i} I(q,p_i,t) + f(\|q-p_i\|)\frac{\partial I(q,p_i,t)}{\partial p_i}. \tag{16}$$

We choose (13) to be a *Lyapunov* function candidate. Calculating the derivative of $\mathcal{W}(P)$ along the trajectories of the system we obtain

$$\begin{aligned}\dot{\mathcal{W}}(P) &= \frac{\partial \mathcal{W}(P)}{\partial p_i}\dot{p}_i + \frac{\partial \mathcal{W}(P)}{\partial t} \\ &= \Big[\int_{V_i(P)} \frac{\partial f(\|q-p_i\|)}{\partial p_i} I(q,p_i,t)\mathrm{d}q + \int_{V_i(P)} f(\|q-p_i\|)\frac{\partial I(q,p_i,t)}{\partial p_i}\mathrm{d}q\Big]\cdot \dot{p}_i \\ &\quad + \int_{V_i(P)} f(\|q-p_i\|)\frac{\partial I(q,p_i,t)}{\partial t}\mathrm{d}q.\end{aligned} \tag{17}$$

Substituting (15) into (17), the derivative along the trajectories of the system becomes

$$\dot{\mathcal{W}}(P) = -\Big[\int_{V_i(P)} \frac{\partial f(\|q-p_i\|)}{\partial p_i} I(q,p_i,t)\mathrm{d}q + \int_{V_i(P)} f(\|q-p_i\|)\frac{\partial I(q,p_i,t)}{\partial p_i}\mathrm{d}q\Big]^2 + \int_{V_i(P)} f(\|q-p_i\|)\frac{\partial I(q,p_i,t)}{\partial t}\mathrm{d}q.$$

We establish our main result by contradiction: assume that the system does not stabilize to the configurations where

$$\frac{\partial I(q,p_i,t)f(\|q-p_i\|)}{\partial p_i} = 0.$$

Then given

$$\lim_{t\to\infty}\frac{\partial I(q,p_i,t)}{\partial t} = 0$$

by Lemma 6.1, after sufficient time T there will be an $\varepsilon > 0$ such that

$$\left|\frac{\partial(I(q,p_i,t)f(\|q-p_i\|)}{\partial p_i}\right| > \varepsilon \quad \forall t > T.$$

It follows that

$$\Big[\int_{V_i(P)}\left|\frac{\partial f(\|q-p_i\|)}{\partial p_i} I(q,p_i,t)\right|\mathrm{d}q + \int_{V_i(P)}\left|f(\|q-p_i\|)\frac{\partial I(q,p_i,t)}{\partial p_i}\right|\mathrm{d}q\Big]^2 > \int_{V_i(P)}\varepsilon^2\mathrm{d}q.$$

Define the following functions:

$$\begin{aligned}W_3(\varepsilon) &\triangleq \int_{V_i(P)}\varepsilon^2\mathrm{d}q, \\ \beta(t) &\triangleq \int_{V_i(P)} f(\|q-p_i\|)\frac{\partial I(q,p_i,t)}{\partial t}\mathrm{d}q.\end{aligned}$$

The derivative of $\mathcal{W}$ along the trajectories of the system can now be bounded as follows

$$\dot{\mathcal{W}}(P) \le -W_3(\varepsilon) + \beta(t) \le -(1-\theta)W_3(\varepsilon) - \theta W_3(\varepsilon) + \beta(t). \tag{18}$$

Looking at the last two terms in the right hand side of (18), and knowing that

$$\lim_{t\to\infty}\frac{\partial I(q,p_i,t)}{\partial t} = 0,$$

we conclude that

$$\lim_{t\to\infty}\int_{V_i(P)} f(\|q-p_i\|)\frac{\partial I(q,p_i,t)}{\partial t}\mathrm{d}q = 0.$$

Since W_3 is a strictly increasing function, there exists a time τ such that $-\theta W_3(\varepsilon)+\beta(t)\leq 0 \quad \forall t>\tau$. After time τ, $\dot{\mathcal{W}}(P)\leq -(1-\theta)W_3(\varepsilon)\triangleq\dot{\gamma}(t)$. Notice that $\dot{\gamma}(t)$ is a constant because it only depends on ε. Therefore we can directly integrate for $\gamma(t)$ as follows $\gamma(t)=\gamma(0)-(1-\theta)W_3(\varepsilon)t$. From the Comparison Lemma (Khalil, 2000) it follows that

$$\mathcal{W}(P)\leq\gamma(t).$$

This implies that there exists a finite time where $\mathcal{W}(P)<0$. But this is a contradiction, since by construction $\mathcal{W}(P)\geq 0$. Hence the assumption that system does not stabilize is invalid; the system indeed converges to configurations where

$$\frac{\partial I(q,p_i,t)f(\|q-p_i\|)}{\partial p_i}=0. \tag{19}$$

□

7 Discussion

In Section 6, the stability of the closed loop system (14)-(15) is established. However, the information surfing control strategy of equation (15) does not directly guarantee the global optimization of sensor information flow, since the set of possible equilibrium points includes all local maxima and minima of $I(q,p_i,t)f(\|q-p_i\|)$.

Nevertheless, efficiency and performance are not compromised. For in the case of local maxima, and with no control input given to the robot, it continues to take measurements at its current location. Because measurements are continuously being taken, the mutual information at that location drops, the information gradient in this area changes, and eventually the robot finds a direction of motion.

In the case of local minima, the robot does have good motion directions, but none of them stands out, and it is uncertain if more measurements can identify a single direction through the mutual information gradient. In this case, it is the group synergy that comes to the rescue: the motion of other robots and their distributed measurements inevitably change the shape of the mutual information distribution, making the local minimum at which one robot may be trapped "erode" with time. Therefore with a multiple robot approach and a shared density function, the likelihood of a robot getting stuck and remaining stuck is significantly reduced compared to the case of a single robot.

Thus, and due to the time-asymptotic properties of mutual information, no local extremum is a positively invariant configuration for the system. The distributed nature of our algorithm in conjunction with sharing of information on the evolution of the density function, establishes a synergy between mobile sensors: in our multi-agent information surfing strategy the *whole is more than the sum of its parts.*

References

Boothby, W. M. (1986). *An Introduction to Differentiable Manifolds and Riemannian Geometry*. Academic Press Inc., 2nd edition.

Burgard, W., Moors, M., Fox, D., Simmons, R., and Thrun, S. (2000). Collaborative multi-robot exploration. In *IEEE International Conference on Robotics and Automation*, pages 476–481.

Cortes, J. and Bullo, F. (2005). Coordination and geometric optimization via distributed dynamical systems. *SIAM Journal on Control and Optimization*, 44(5):1543–1574.

Cortes, J., Martinez, S., and Bullo, F. (2005). Spatially-distributed converage optimization and control with limited-range interactions. *ESIAM: Control, Optimization and Calculus of Variations*, 11(4):691–719.

Cortez, A. R., Papageorgiou, X., Tanner, H. G., Klimenko, A. V., Hengarter, N., Borozdin, K. N., and Priedhorsky, W. C. (2007). Smart radiation sensor management: Nuclear search and mapping using mobile robots. *IEEE Robotics and Automation Magazine*. (submitted).

Cover, T. M. and Thomas, J. A. (1991). *Elements of Information Theory*. Wiley-Interscience.

Elfes, A. (1989). *Occupancy grids: A probabilistic framework for robot perception and navigation*. PhD thesis, Carnegie Mellon University.

Grabowski, R., Navarro-Serment, L. E., Paredis, C. J., and Khosla, P. K. (2000). Heterogeneous teams of modular robot for mapping and exploration. *Autonomous Robots*, 8(3):293–308.

Grocholsky, B., Keller, J., Kumar, V., and Pappas, G. (2006). Cooperative air and ground surveillance. *IEEE Robotics and Automation Magazine*, pages 16–26.

Hussein, I. I. and Stipanovic, D. M. (2006). Effective coverage control for mobile sensor networks. In *IEEE Confrence on Decision and Control*, pages 2747–2752.

Khalil, H. K. (2000). *Nonlinear Systems*. Prentice-Hall, 3rd edition.

Klimenko, A., Priedhorsky, W. C., Hegartner, N., and Borozdin, K. N. (2006). Efficient strategies for low-statistics nuclear searches. *IEEE Transactions on Nuclear Science*, 53(3):1435–1442.

Lilienthal, A. and Duckett, T. (2004). Building gas concentration gridmaps with a mobile robot. *Robotics and Autonomous Systems*, 48(1):3–16.

Lindhe, M., Orgen, P., and Johansson, K. H. (2005). Flocking with obstacle avoidance: A new distributed coordination algorithm based on voronoi partitions. In *IEEE International Confrence on Robotics and Automation*, pages 1785–1790.

Martinez, S., Cortes, J., and Bullo, F. (2007). Motion coordination with distributed information. *IEEE Control Systems Magazine*. (to appear).

Moorehead, S. J. (2001). *Autonomous Surface Exploration for*. PhD thesis, Carnegie Mellon University, 5000 Forbes Avenue, Pittsburgh, Pennsylvania 15213.

Moravec, H. P. (1988). Sensor fusion in certainty grids for mobile robots. *AI Magazine*, 9(2):61–74.

Nemzek, R. J., Dreicer, J. S., Torney, D. C., and Warnock, T. T. (2004). Distributed sensor networks for detection of mobile radioactive sources. *IEEE Transactions on Nuclear Science*, 51(4):1693–1700.

Orgen, P., Fiorelli, E., and Leonard, N. E. (2004). Cooperative control of mobile sensor networks: Adaptive gradient climbing in a distributed environment. *IEEE Transactions on Automatic Control*, 49(8):1292–1302.

Popa, D. O., Stephanou, H. E., Helm, C., and Sanderson, A. C. (2004). Robotic deployment of sensor networks using potential fields. In *IEEE International Conference on Robotics and Automation*, pages 642–647.

Reza, F. M. (1994). *An Introduction To Information Theory*. Dover Publications Inc.

Thrun, S. (2001). A probabilistic on-line mapping algorithm for teams of mobile robots. *The International Journal of Robotics Research*, 20(5):335–363.

Yamauchi, B. (1998). Frontier-based exploration using multiple robots. In *Second International Conference on Autonomous Agents*, pages 47–53.

A Proof of Lemma 6.1

Taking the mutual information defined in equation (11), we find its time derivative to be

$$\frac{\partial I(q,p_i,t)}{\partial t} = \frac{\partial h}{\partial d}\frac{\partial d}{\partial t}.$$

The first partial derivative takes the form

$$\frac{\partial h}{\partial d} = \sum_{i=1}^{12} A_i, \tag{20}$$

where A_1 through A_{12} are fractional terms that make up the whole expression. For the first term

$$A_1 \triangleq \frac{(-1-c)\Gamma(1+c,\alpha_1 \cdot d \cdot \chi)^2}{(1+c)d \cdot c!(\Gamma(1+c,\alpha_1 \cdot d \cdot \chi) - \Gamma(1+c,\alpha_1 \cdot d \cdot \chi)^2))\log 2},$$

we find that

$$\lim_{d\to\infty} A_1 = 0,$$

due to having $c!$ in the denominator, which is the total number of radiation counts collected during the mission. Notice that the total number of counts c, grows much faster than d does, because of the added effect of background

radiation and source. Other terms that show this same behavior are:

$$A_2 = \frac{(-1-c)\Gamma(1+c,\alpha_2\cdot d\cdot\chi)^2}{(1+c)d\cdot c!(\Gamma(1+c,\alpha_2\cdot d\cdot\chi)-\Gamma(1+c,\alpha_1\cdot d\cdot\chi)^2))\log 2},$$

$$A_3 = \frac{((-1-c)e^{(-\alpha_1\alpha_2)d\chi}\Gamma(1+c,\alpha_1 d\chi)(\alpha_1 d e^{\alpha_2 d\chi}\chi(\alpha_1 d\chi)^c(1+\alpha_1 d\chi\Gamma(1+c)-2e^{(-\alpha_1-\alpha_2)d\chi}\Gamma(1+c,\alpha_2 d\chi))))}{(1+c)d\cdot c!(\Gamma(1+c,\alpha_2\cdot d\cdot\chi)-\Gamma(1+c,\alpha_1\cdot d\cdot\chi)^2))\log 2},$$

$$A_4 = \frac{(\alpha_1(-1-c)e^{(-\alpha_1-\alpha_2)d\chi+\alpha_2 d\chi}\chi(\alpha_1 d\chi)^c\Gamma(2+c)(\Gamma(2+c,\alpha_1 d\chi)-\Gamma(2+c,\alpha_2 d\chi)+c\Gamma(1+c)\log(\frac{\alpha_1}{\alpha_2})))}{(1+c)d\cdot c!(\Gamma(1+c,\alpha_2\cdot d\cdot\chi)-\Gamma(1+c,\alpha_1\cdot d\cdot\chi)^2))\log 2},$$

$$A_5 = (\alpha_2 d\chi)\frac{\alpha_2(-1-c)e^{(-\alpha_1-\alpha_2)d\chi+\alpha_1 d\chi}\chi(1+c+\alpha_2 d\chi\Gamma(2+c))\Gamma(1+c,\alpha_2 d,\chi)}{(1+c)d\cdot c!(\Gamma(1+c,\alpha_2\cdot d\cdot\chi)-\Gamma(1+c,\alpha_1\cdot d\cdot\chi)^2))\log 2},$$

$$A_6 = (\alpha_2 d\chi)\frac{\alpha_2(-1-c)e^{(-\alpha_1-\alpha_2)d\chi+\alpha_1 d\chi}\chi\Gamma(2+c)\Gamma(2+c,\alpha_1 d,\chi)}{(1+c)d\cdot c!(\Gamma(1+c,\alpha_2\cdot d\cdot\chi)-\Gamma(1+c,\alpha_1\cdot d\cdot\chi)^2))\log 2},$$

$$A_7 = (\alpha_2 d\chi)\frac{\alpha_2(-1-c)e^{(-\alpha_1-\alpha_2)d\chi+\alpha_1 d\chi}\chi\Gamma(1+c,\alpha_1 d\chi)(1+c+\Gamma(2+c)(\alpha_1 d\chi+Log(\frac{e^{-\alpha_1 d\chi}(\alpha_1 d\chi)^c}{e^{-\alpha_2 d\chi}(\alpha_2 d\chi)^c})}{(1+c)d\cdot c!(\Gamma(1+c,\alpha_2\cdot d\cdot\chi)-\Gamma(1+c,\alpha_1\cdot d\cdot\chi)^2))Log(2)},$$

$$A_8 = (\alpha_2 d\chi)\frac{\alpha_1(-1-c)e^{(-\alpha_1-\alpha_2)d\chi+\alpha_2 d\chi}\chi\Gamma(1+c,\alpha_2 d\chi)(1+c+\Gamma(2+c)(\alpha_1 d\chi+\log(\frac{e^{-\alpha_2 d\chi}(\alpha_2 d\chi)^c}{e^{-\alpha_1 d\chi}(\alpha_1 d\chi)^c})}{(1+c)d\cdot c!(\Gamma(1+c,\alpha_2\cdot d\cdot\chi)-\Gamma(1+c,\alpha_1\cdot d\cdot\chi)^2))\log 2}.$$

The last four terms that make up (20) are the ones that involve the generalized hypergeometric function:

$$A_9 = \frac{\alpha_1^2 cde^{(-\alpha_1-\alpha_2)d\chi+\alpha_2 d\chi}\chi^2(\alpha_1 d\chi)^{2c}\Omega(1+c,1+c,2+c,2+c,-\alpha_1 d\chi)}{(1+c)^2(\Gamma(1+c,\alpha_1 d\chi)-\Gamma(1+c,\alpha_2 d\chi))^2\log 2},$$

$$A_{10} = \frac{\alpha_1^2 cde^{(-\alpha_1-\alpha_2)d\chi+\alpha_1 d\chi}\chi^2(\alpha_2 d\chi)^{2c}\Omega(1+c,1+c,2+c,2+c,-\alpha_2 d\chi)}{(1+c)^2(\Gamma(1+c,\alpha_1 d\chi)-\Gamma(1+c,\alpha_2 d\chi))^2\log 2},$$

$$A_{11} = \frac{(\alpha_1\alpha_2 cde^{(-\alpha_1-\alpha_2)d\chi+\alpha_1 d\chi}\chi^2(\alpha_1 d\chi)^c\Omega(1+c,1+c,2+c,2+c,-\alpha_1 d\chi))}{(1+c)^2(\Gamma(1+c,\alpha_1 d\chi)-\Gamma(1+c,\alpha_2 d\chi))^2\log 2},$$

$$A_{12} = \frac{(\alpha_1\alpha_2 cde^{(-\alpha_1-\alpha_2)d\chi+\alpha_2 d\chi}\chi^2(\alpha_1 d\chi)^c\Omega(1+c,1+c,2+c,2+c,-\alpha_2 d\chi))}{(1+c)^2(\Gamma(1+c,\alpha_1 d\chi)-\Gamma(1+c,\alpha_2 d\chi))^2\log 2}.$$

Recall that the generalized hypergeometric function Ω is defined as

$$\Omega(1+c,1+c,2+c,2+c,-\alpha_1 d\chi) = \sum_{n=0}^{\infty}\frac{(1+c)_n(1+c)_n}{(2+c)_n(2+c)_n}\cdot\frac{-\alpha_1^n}{n!},$$

where $(1+c)_n = (1+c)(1+c+1)(1+c+2)\cdots(c+n)$. This function exhibits oscillatory behavior with n, and because of this the net effect is

$$\Omega(1+c,1+c,2+c,2+c,-\alpha_1 d\chi) = 0.$$

In fact, any reasonably large finite term approximation of Ω will yield outcomes that are numerically insignificant. For this reason, we get no contribution from the terms A_9 through A_{12}, and (20) becomes

$$\frac{\partial h}{\partial d} = \sum_{i=1}^{8} A_i.$$

Note now, that for all terms A_1 through A_8 it holds

$$\lim_{d\to\infty}\frac{\partial h}{\partial d} = 0,$$

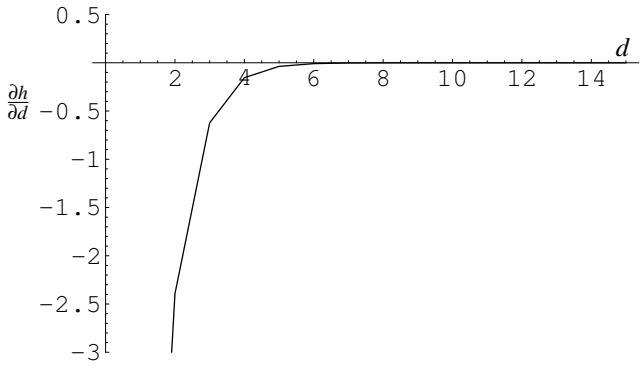

Figure 4: The behavior of $\frac{\partial h}{\partial d}$ as d grows large, under the conditions: $\alpha_1 = 1$ cts/s, $\alpha_2 = 10$ cts/s, $\chi = 1$ cm, $c = 2d$.

and with c growing much faster than time (even in the case of only background radiation),

$$\lim_{t\to\infty} \frac{\partial I(q, p_i, t)}{\partial t} = \lim_{t\to\infty} \frac{\partial h}{\partial d} \frac{\partial d}{\partial t} = 0.$$

This asymptotic analysis is verified in plots of the rate of change of the entropy, as a function of variable d, as shown in Figure 4.